SYNTHETIC MODULATED STRUCTURES

Edited by

LEROY L. CHANG

IBM Thomas J. Watson Research Center
Yorktown Heights, New York

B. C. GIESSEN

Department of Chemistry
Northeastern University
Boston, Massachusetts

1985

ACADEMIC PRESS, INC.
(Harcourt Brace Jovanovich, Publishers)
Orlando San Diego New York London
Toronto Montreal Sydney Tokyo

9 ELECTRONIC AND MAGNETIC PROPERTIES OF METALLIC SUPERLATTICES

Charles M. Falco

Departments of Physics and of Optical Sciences and Arizona Research Laboratories
The University of Arizona
Tucson, Arizona

Ivan K. Schuller

Materials Science and Technology Division
Argonne National Laboratory
Argonne, Illinois

I. INTRODUCTION

Early work on artificially layered metals was initiated by DuMond and Youtz (1940) to produce layered structures for x-ray diffraction gratings. This goal, as well as producing polarizers and monochromators for neutrons [see Spiller (1981) and references cited therein, also Barbee in the same volume], has motivated a number of workers (Saxena and Schoenborn, 1977a,b; Hamelin, 1976; Lynn *et al.*, 1976). It was very early discovered that interdiffusion greatly affected the structures produced, and many workers have concentrated on these materials for the study of the physics of diffusion (Dinklage, 1967; Dinklage and Frerichs, 1963; Cook and Hilliard, 1969; Berry and Pritchet, 1976; Paulson and Hilliard, 1977; Roll and Reill, 1982). However, as described in several other

ISBN 0-12-170470-X

chapters in this volume, advances in thin-film-deposition technology have motivated interest in artificially prepared materials exhibiting different physical properties than those that occur naturally. This chapter will review work on the electronic transport properties and magnetic properties of artificially layered metals.

II. SAMPLE PREPARATION

By far the greatest amount of published electrical transport properties data is on the Nb–Cu system. The various groups (Schuller and Falco, 1980; Geerk *et al.*, 1982, Lowe *et al.*, 1981) reporting some results on this material all used the same sputtering technique for producing samples. In this technique single-crystal substrates (Schuller and Falco, 1980; Falco and Schuller, 1982a; Geerk *et al.*, 1982; Lowe *et al.*, 1981) or amorphous Kapton tape (Lowe *et al.*, 1982) are placed in a platform that can be rotated at a precisely controlled speed either above (sputter-up configuration) or below (sputter-down configuration) the Nb and Cu sputtering sources. This is shown schematically in Fig. 1. By varying the rotation speed, as well as the sputtering rates, samples of individual layer thickness in the range $\sim 5-5000$ Å have been prepared. Typically samples with total film thickness of ~ 1 μm are used for transport properties measurements. One disadvantage of this sputtering technique is that argon gas pressures of $\sim 1 \times 10^{-3}$ to 2×10^{-2} torr are necessary during the deposition so that no *in situ* surface characterization probes can be used to monitor the growth during deposition.

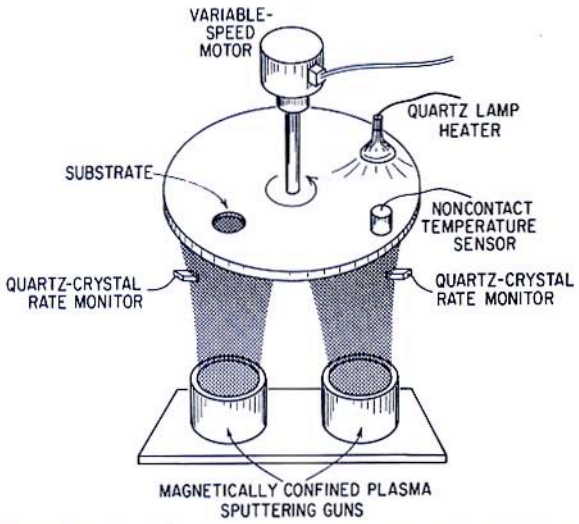

Fig. 1. Schematic diagram of typical sputtering system used to prepare metallic superlattices.

In one case (Nb–Ta) metallic superlattices have also reportly been grown by conventional evaporation in a ultrahigh vacuum (UHV) system at 4×10^{-9} torr (Durbin *et al.*, 1981, 1982). In that case, the substrates were kept fixed on a heated platform (700–900°C) while two electron-beam ovens were alternately shuttered to produce the layered structure. This technique has the advantage that the UHV environment allows the use of surface probes during growth, although growth rates are lower (0.1–10 Å/sec) compared to sputtering (10–200 Å/sec).

III. X-RAY CHARACTERIZATION

A knowledge of the structure of the multilayer films is essential in order to correlate with measured electronic or magnetic properties. We will address here only the x-ray characterization of those materials whose electronic properties have been measured in some detail. This is of importance since some electronic properties have been found to be intimately related to the structural characteristics. Detailed studies (Lowe *et al.*, 1981; Schuller, 1980) of the x-ray diffraction data from Nb–Cu samples grown by several groups (Schuller and Falco, 1980; Geerk, 1982; Lowe, *et al.*, 1981) show that for layer thicknesses greater than 10 Å the samples have long-range structural coherence perpendicular to the layers (z coherent). A lower limit on this perpendicular structural coherence length of ~200 Å can be placed by the x-ray measurements. In the plane of the sample the crystallite size is limited to ~150–200 Å.

An alternate, x-ray method for the determination of the layer thickness relies on small angle scattering around $\theta = 0°$. This method is based on the direct scattering by the difference in x-ray refractive index of the two constituents. The advantage of such a method is that the layer thickness can be determined even for constituents formed of amorphous–amorphous and crystalline–amorphous materials and does not require z coherence. However, this method gives no information regarding the crystal structure and interatomic spacing within each layer. This type of x-ray scattering has been the basis for the production of neutron reflectors (Saxena and Schoenborn, 1977a,b; Hamelin, 1976; Lynn *et al.*, 1976).

For z-coherent samples with layer thicknesses in the range 10–100 Å, the x-ray diffraction patterns show a series of superlattice lines due to the constructive and destructive interference of the x rays by the coherent registry of sequential layers of the sample. This is shown in Fig. 2. The spacing of these superlattice lines can be directly used to determine the layer thickness since (Schuller, 1980)

$$\Lambda = \lambda_x / 2(\sin \theta_i - \sin \theta_{i+1}), \tag{1}$$

where Λ is the superlattice wavelength, λ_x is the x-ray wavelength, and i and

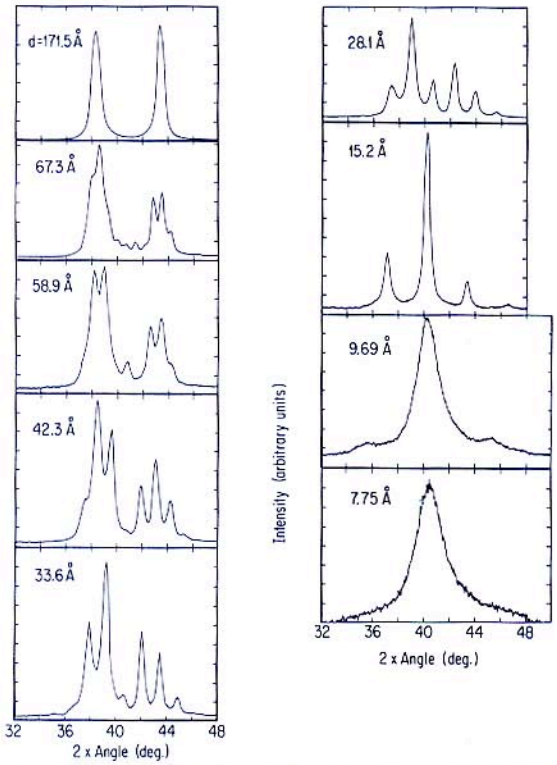

Fig. 2. Bragg x-ray diffraction data for a series of Nb–Cu samples of different layer thicknesses d.

$i+1$ refer the adjacent diffraction peaks in the $\theta-2\theta$ scan. For thicker layers, the spacing of the superlattice lines decreases, until at about $d \cong 100$ Å they merge with the Cu (111) and Nb (110) x-ray peaks. Because of this, for layer thicknesses beyond this point x rays can no longer be used to determine layer thickness. Two other independent methods are (a) using the size of the particle beam in conjunction with the sputtering rate and the rotation speed to determine a layer thickness and (b) measuring the total thickness and dividing by the total number of revolutions to determine a layer thickness. These four independent methods agree to within 5% in the common thickness range (Schuller and Falco, 1982) and thus any of the methods can be used.

One group has studied Nb–Cu for very thin layers (Werner *et al.*, 1982). Below 10 Å the material becomes progressively more disordered, causing the x-ray linewidths to greatly increase; however, in this regime the layer thickness as determined from the sputtering geometry and rate remains a good parameter for characterizing the elastic electron mean free path.

Extensive x-ray measurements (Durbin *et al.*, 1982) have also been reported on Nb–Ta multilayers. These samples were grown on several substrates in a variety of crystallographic orientations. Structural coherence distances were derived from x-ray rocking curves and in the next section are compared with electron mean free paths determined from resistivity measurements. X-ray measurements were also used to establish that the Nb and Ta interdiffuse over several lattice planes about each interface in the Nb (28-Å)–Ta (22-Å) samples. Durbin *et al.* (1982) concluded from these measurements that "it does not appear possible to choose a growth temperature and (convenient) evaporation rate such that the interfaces remain sharp while the growth perfection (as determined by x-ray rocking curves) remains satisfactory." If an alternate growth technique (such as sputtering) is not found for this material, the diffuseness of the interfaces will limit the growth of this material to layer thickness of $\gtrsim 10-15$ Å. This same diffuseness may also prohibit the observation of superlattice effects in the electronic properties of Nb–Ta.

Work on producing Nb–Ta multilayers by sputtering has also found interdiffusion at the interfaces (Hertel *et al.*, 1982). In this case, samples grown at temperatures of $>810°C$ were found to interdiffuse over at least 8.5 Å. Samples grown at temperatures of $<810°C$ were found to be polycrystalline. Further work is necessary to find whether a suitable growth temperature along with appropriate sputtering parameters can be found that gives sharp interfaces and crystalline samples.

IV. ELECTRICAL TRANSPORT

A. Resistivity

Figure 3 shows a plot of the low-temperature (20-K) resistivity ρ versus layer thickness for a series of 25 Nb–Cu samples grown in random order over a period of one year (Werner *et al.*, 1982; Falco and Schuller, 1982b). Below approximately 10-Å layer thickness the resistivity saturates close to the Ioffe–Regel (1960) limit of ~ 150 μohm cm. Above this thickness the resistivity is inversely proportional to the layer thickness as would be predicted for a mean free path that is limited by boundary scattering at the layers. As can be seen from Fig. 4, for very thick layers the resistivity approaches the value expected for bulk Cu and Nb films in parallel. The arrows in Fig. 4 indicate the measured resistivities for ~ 1-μm-thick pure Cu and Nb film grown under the same sputtering conditions as were the layered samples. Also shown is the expected result for Nb and Cu films connected in parallel; corrected by the appropriate geometrical factor of 2 since the individual layer thickness is half the total sample thickness. It should be emphasized that the value of such resistivity measurements should not be underestimated since the electronic mean free path will determine whether superlattice effects on the band structure are likely to be observed.

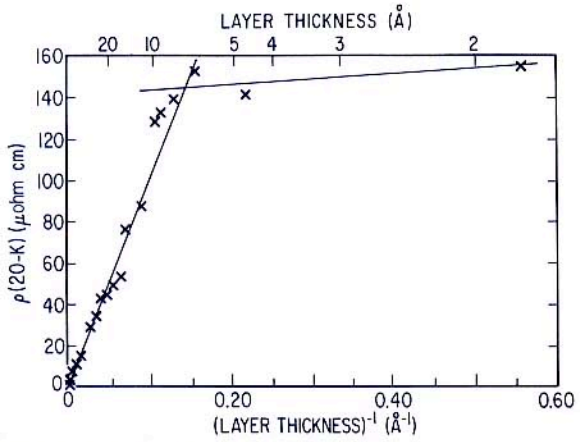

Fig. 3. Resistivity at 20 K versus inverse layer thickness for a series of Nb–Cu samples (Werner *et al.*, 1982).

Since resistivity is expected to scale approximately as the inverse of layer thickness, a useful way to present these data is in a plot of resistivity times layer thickness versus layer thickness. Figure 5 is a plot of $2\rho d$ versus $2d$ for published Nb–Cu data from two groups (Lowe *et al.*, 1981; Werner *et al.*, 1982). Log–log scales are used for convenience in presentation; with the solid curve being a straight line on a linear plot. This straight line behavior is predicted for a mean free path proportional to layer thickness (Mayadas and Shatzkes, 1970). Resis-

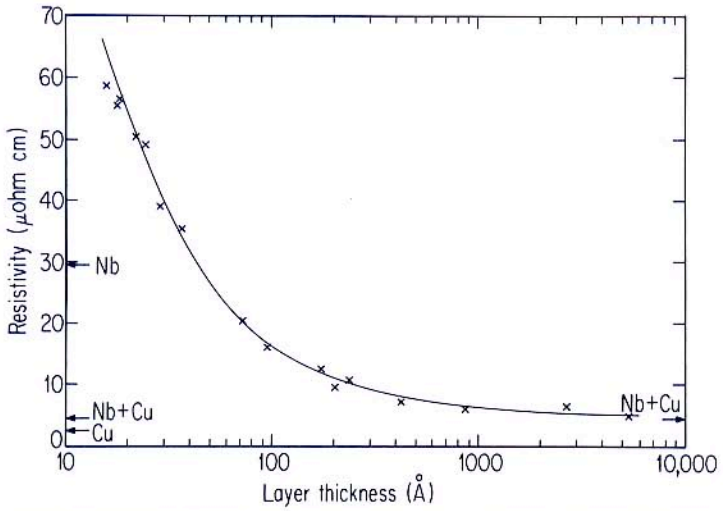

Fig. 4. Room-temperature resistivity for a series of Nb–Cu samples versus layer thickness at 295 K.

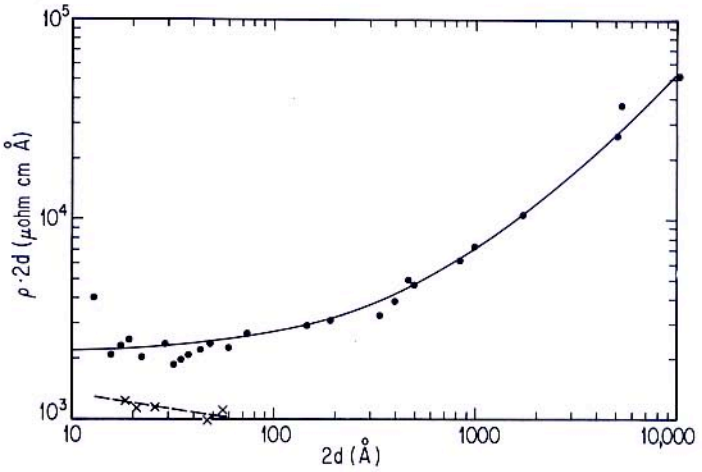

Fig. 5. Resistivity times the bilayer thickness versus bilayer thickness for Nb–Cu samples. [●, from Werner *et al.* 1982; ×, from Lowe *et al.* (1981).]

tivity data on Nb–Ge (Ruggiero, 1981) have not been plotted on this figure since the "spacer" material (Cu in one case and Ge in the other) is considerably different. The data of Lowe *et al.* (1982) in Fig. 6, which shows ρ increasing as d is decreased, perhaps imply increasing amounts of disorder for these particular films, causing ρ to increase faster than d^{-1}. Published values of the superconducting transition temperatures for these Nb–Cu films (Lowe *et al.*, 1981) are much lower than those samples that follow the solid line (Banerjee *et al.*, 1982). This is also consistent with larger amounts of disorder or the presence of impurities.

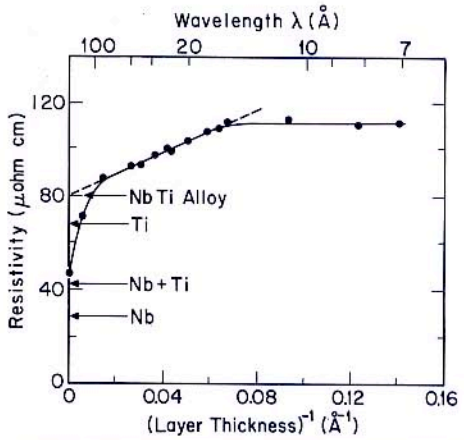

Fig. 6. Resistivity versus inverse layer thickness for a series of Nb–Ti samples.

The behavior of resistivity shown in Figs. 4 and 5 is not unique to Nb–Cu, although there can be differences in details for different materials as discussed below. Figure 6 shows the measured room-temperature resistivity of a series of Nb–Ti samples (Zheng *et al.*, 1981b). In this case the resistivity begins to saturate for ~15-Å layer thicknesses at 115 μohm cm (slightly lower than the case of Nb–Cu although close to values expected from the Ioffe–Regel criterion). For slightly thicker layers the resistivity scales as the inverse of the layer thickness just as it did for Nb–Cu. However, the value of 80 μohm cm obtained by extrapolating to infinite layer thickness is identical to that of a uniform Nb–Ti alloy. This is easily understood since the equilibrium binary phase diagram for Nb–Ti, unlike Nb–Cu, shows that the two materials form continuous sets of solid solutions. [These and other binary phase diagrams can be found in Hansen and Anderk (1958), Elliott (1965), Shunk (1969), and Moffatt (1981).] Thus in this regime of layer thickness there is probably considerable interdiffusion contributing both to the elastic mean free path and causing the "background" resistivity to be that of the uniform alloy. Finally, for layers thicker than ~100 Å in which any contribution from interdiffusion at the interfaces becomes negligible, the resistivity approaches that expected of thick Nb and Ti slabs in parallel.

Mean free path results obtained from resistivity measurements have also been reported for several Nb–Ta superlattices of unequal layer thickness (Durbin *et al.*, 1982) (Nb, 28 Å; Ta, 22 Å). However, as shown in Fig. 7, the reported mean free paths do not scale with the structural coherence distance (derived from x-ray rocking curves). The arrow in Fig. 7 denotes the meanfree path of a

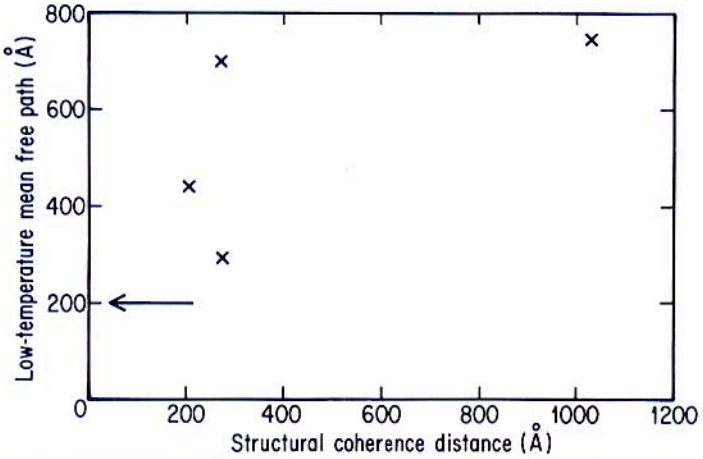

Fig. 7. Low-temperature electronic mean free path versus structural coherence distance determined from x-ray measurements for four Nb–Ta superlattices. [Data taken from Durbin *et al.* (1982).]

"disordered $Nb_{0.47}-Ta_{0.53}$ alloy" (Calverly and Rose-Innes, 1960). Within the uncertainties of the assumptions in determining the mean free path from the resistivity, this value is essentially the same as reported (Durbin *et al.*, 1982) for Nb–Ta superlattices. Without a detailed study of ρ versus d for this material, it is hard to reconcile these observations, as well as to predict whether Nb–Ta films produced in this way can be of sufficient perfection to expect superlattice effects on the electronic properties.

B. Temperature Dependence of the Resistivity

Figure 8 shows the temperature-dependent part of the resistivity versus layer thickness for a series of Nb–Cu samples (Werner *et al.*, 1982). Even in the region below 10 Å, in which the x-ray measurements (Schuller, 1980) (Fig. 2) show this material to be becoming progressively more disordered, the systematic way in which the resistivity changes with layer thickness (determined by using the preparation parameters) shows that it is meaningful to use the substrate platform rotation speed (see Fig. 1) as an indication of the elastic mean free path. While the layer thickness serves as a useful parameter for characterizing the mean free path, in this regime of very short mean free paths the results are independent of the exact structure of the film. All that is important is the fact that it is possible to control artificially the resistivity (i.e., elastic mean free path) of the films by the deposition process.

At any arbitrary fixed temperature in the range $20\ K < T < 300\ K$, the temperature coefficient of resistivity (TCR) for these Nb–Cu samples shows a rather sudden change from positive (metallic) to negative (nonmetallic) as a function of mean free path (Werner *et al.*, 1982). This is shown in Fig. 9, in which $d\rho/dT$ versus layer thickness is plotted at three temperatures. This

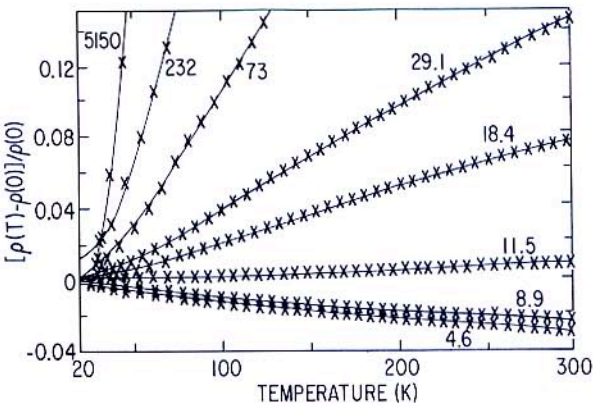

Fig. 8. Temperature-dependent part of the resistivity versus temperature for a series of Nb–Cu samples of various layer thicknesses d (labeled in angstroms on the curves) (Werner *et al.*, 1982).

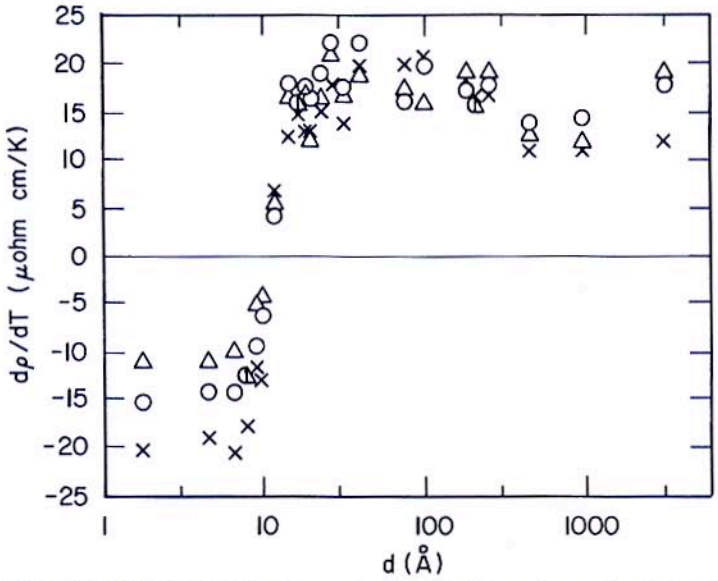

Fig. 9. Plot of $d\rho/dT$ at three temperatures versus layer thickness for a series of Nb–Cu samples (Werner *et al.*, 1982). (△, 250 K; ○, 150 K; ×, 50 K.)

change from positive to negative TCR occurs for a mean free path that is decreased by only 2 or 3 atomic spacings (~5–6 Å).

The point at which the TCR passes through zero has a very useful application. Because $d\rho/dT$ is very weakly dependent on temperature, for a sample of appropriate layer thickness ($d \cong 10$ Å) the TCR can be made to be less than 8 ppm/K over the entire temperature range 300–3 K (at which point the sample becomes superconducting). Thus one can fabricate materials for thin-film resistors that are extremely stable against temperature fluctuations or drifts.

The temperature dependence of the conductivity of a material in the nonmetallic regime (negative TCR) has been the subject of extensive theoretical investigation. [For a review of the experimental and theoretical situation, see Dynes (1982); also, Abrahams *et al.* (1979), Altshuller and Aronov (1979), and Kaveh and Mott (1981, and references cited therein).] It has been shown that due to electron–electron interaction effects (Altshuller and Aronov, 1979) or localization (Abrahams *et al.*, 1979), the temperature-dependent part of electrical conductivity can be written

$$\frac{\delta\sigma}{\sigma} = 1 - \left(\frac{3}{2x}\right) \ln(1+x) \left(\frac{1}{N_0\pi^3} \frac{k_B}{(hD)^3}\right)^{1/2} T^{1/2}, \tag{2}$$

where D is the diffusion coefficient for electrons, N_0 is the density of states at the Fermi surface, and $x = (2k_F/\mu)^2$, where k_F is the Fermi momentum and μ is the

inverse screening length. Assuming $\delta\sigma \ll \sigma$, as is observed experimentally in the Nb–Cu samples, and using the Einstein relation $\sigma_0 = N_0 e^2 D_0$ leads to

$$\delta\sigma \cong 1 - \left(\frac{3}{2x}\right) \ln(1+x) \left(\frac{k_B e^4}{\hbar^3 \pi^6}\right)^{1/2} \frac{D_0}{D^{3/2}} T^{1/2}. \tag{3}$$

Figure 10 shows a plot of $\delta\sigma$ versus $T^{1/2}$ for a Nb–Cu sample of layer thickness 9.5 Å (Werner *et al.*, 1982). This is just slightly into the negative TCR regime, as seen from Fig. 10. Above ~ 35 K the temperature dependence is well described by Eq. (3) with a temperature-independent diffusion coefficient D. Similar behavior was reported for all five other Nb–Cu samples that exhibit a negative TCR. However, it should be noted that in the same temperature region the dependence $\exp(-B/T^{1/4})$ predicted by Mott's variable-range hopping model (Mott, 1969) cannot be distinguished from the $T^{1/2}$ dependence predicted by localization and electron–electron correlation theories. Fits to a number of other dependences have been tried, but no other theoretical expression has been found to fit the experimental results.

The prefactor to the $T^{1/2}$ term in Eq. (3) can be extracted from a plot similar to Fig. 10. The diffusion coefficient D_0 can also be obtained from the Einstein relation and the extrapolated zero temperature conductivity σ_0. Comparing these two quantities leads to $1 - (3/2x)\ln(1+x) \cong 10^{-2}$. Solving for x leads to $k_F/\mu \cong \frac{1}{2}$, implying that both localization and electron–electron correlation effects are important in the Nb–Cu system in this regime when the electron

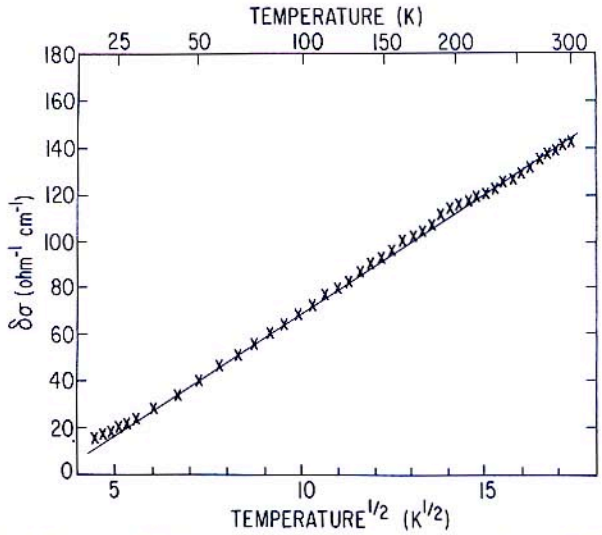

Fig. 10. Plot of $\delta\sigma$ versus $T^{1/2}$ for a Nb–Cu sample of layer thickness 9.5 Å (Werner *et al.*, 1982). Here $\delta\sigma = \sigma(T) - 7762.3$ ohm^{-1} cm^{-1} is the change in conductivity from its value at zero temperature.

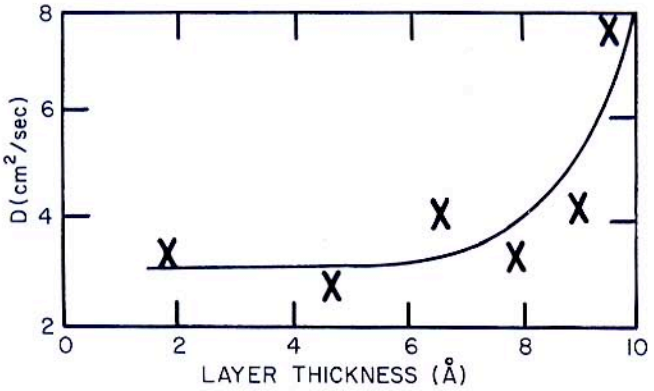

Fig. 11. High-temperature diffusion coefficient D [extracted from Eq. (2)] versus layer thickness for a series of Nb–Cu samples (Werner *et al.*, 1982).

mean free path has been artificially reduced to very small values by the material fabrication process.

It is interesting to note that while the low-temperature diffusion coefficient D_0 obtained from the Einstein relation for these samples is essentially constant (because the conductivities are approximately the same), the high-temperature diffusion constant D is not. The high-temperature diffusion constants extracted from the slope of Eq. (3) increase markedly as the nonmetallic to metallic transition is approached. This is shown in Fig. 11.

C. Correlation of Electrical and Mechanical Properties

Although mechanical properties of artificially layered metals are discussed in detail in other contexts within this volume, at least one such property has been shown to be correlated with an electronic transport property. Since this is the first example observed of such a relationship, we will discuss it here.

Samples of Nb–Cu with individual layers of equal thickness in the range 5 Å to 1 μm were prepared on single-crystal sapphire substrates. Both electrical resistivity and elastic constant measurements were made on the same set of samples. The electrical resistivity was measured by using a four-probe technique over the temperature range 300–10 K. The elastic constants were determined from a Brillouin light-scattering technique at room temperature (Kueny *et al.*, 1982). The details of the experiment are described by Kueny *et al.*, (1982).

A spectrum from one sample is shown in Fig. 12. From such measurements at several values of ω and k, it is possible to obtain the surface sound (Rayleigh) velocity v_R. The measured velocities as a function of twice the layer thickness

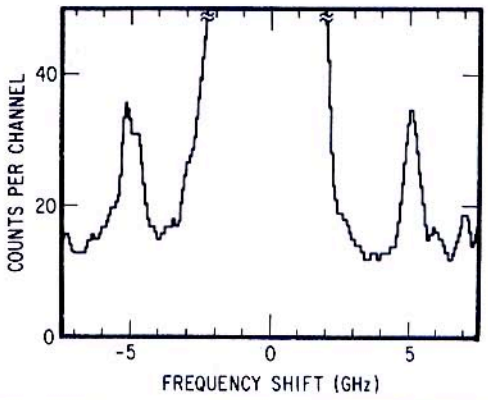

Fig. 12. Brillouin spectrum of a Nb–Cu sample with bilayer thickness 20 Å (Kueny *et al.*, 1982).

are shown in Fig. 13. Note the ~ 20% drop in sound velocities for layer thickness centered around ~ 10 Å. Referring to the temperature derivative of resistivity $d\rho/dT$ shown in Fig. 9, we can see that the minimum in v_s corresponds closely to the point where $d\rho/dT$ undergoes a transition from positive (metallike) to negative (nonmetallic). Thus the structural and electronic properties of these materials are correlated.

For an interpretation of the results of Fig. 13 in terms of elastic constants, the reader is referred to Farnell (1969). In the region in which the wavelength of the phonons probed in these experiments (3000 Å $< \lambda_{\text{phonon}} <$ 4300 Å) is much

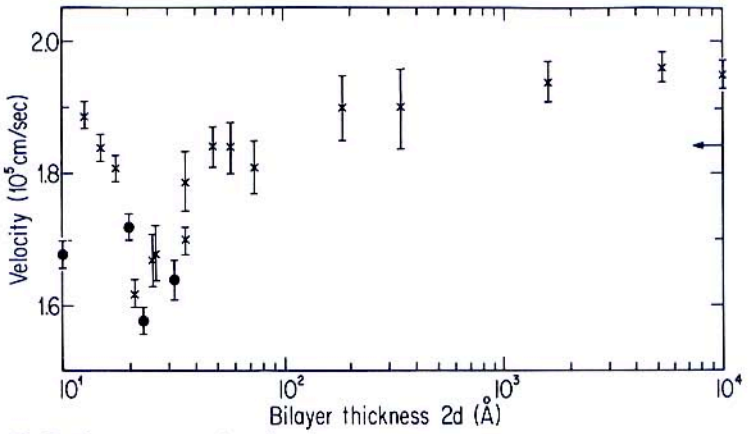

Fig. 13. Surface wave velocity of Nb–Cu superlattices as a function of bilayer thickness. The arrow indicates the calculated velocity for films with bilayer thickness ≲ 100 Å (Kueny *et al.*, 1982).

greater than the bilayer thickness $2d$, the films can be considered to be homogeneous and the velocity of the surface wave is given by (Farnell, 1969)

$$v_R = \beta(C_{44}/\rho_m)^{1/2}, \tag{4}$$

where ρ_m is the mass density of the film and β a rather insensitive function of C_{11}, C_{33}, and C_{13}. Under certain assumptions for the C_{ij}'s, it was found (Kueny *et al.*, 1982) that $0.86 \leq \beta \leq 0.98$. Thus by using Eq. (4) it was concluded that the dominant part of the decrease and subsequent increase in v_R centered about $d = 10$ Å corresponds to a $\sim 35\%$ decrease in C_{44}.

The expected value for v_R, assuming that the Nb and Cu layers kept their bulk properties, can be calculated by following Rytov (1956). Assuming that the β's for Nb and Cu are not very different and making use of the fact that the densities of Nb (8.60 gm/cm) and Cu (8.93 gm/cm) are nearly equal, then

$$v_R^2(\text{Nb–Cu}) \cong 2v_R^2(\text{Cu})v_R^2(\text{Nb})/[v_R^2(\text{Cu}) + v_R^2(\text{Nb})]. \tag{5}$$

For [111] Cu and [110] Nb the calculated velocity $v_R(\text{Nb–Cu}) = 1.84 \times 10^5$ cm/sec, which is shown by the arrow on the right side of Fig. 13. If the artificial layering of this material did not affect the bulk properties of the Cu and Nb layers, this value should be observed for all film for which $2d \ll \lambda_{\text{phonon}}$ since in this case the phonons average over many layers.

Deviations are expected for $2d \gtrsim 1000$ Å since in this case the phonons no longer average over many layers and consequently the topmost layer will dominate in determining the velocity of the surface wave. As can be seen from Fig. 13, in the region $2d = 100 - 1000$ Å there is reasonable agreement between experiment and the calculated $v_R(\text{Nb–Cu})$. For $2d > 1000$ Å the observed value matches the calculated $v_R(\text{Nb})$, which is also expected since for these particular samples the topmost layer was Nb. However, a $\sim 20\%$ dip in v_R occurs between $2d = 100$ and 12.5 Å, which as discussed above is interpreted according to Eq. (4) as a $\sim 35\%$ decrease in C_{44}.

The question remains as to how to explain the observed decrease in C_{44} due to the layering. This dip in the elastic constants might arise from either structural changes that alter the phonon spectrum or changes in the electronic structure (the subject of this chapter). It has been found that the softening of the elastic constant is correlated with an expansion of the average lattice spacing (Khan *et al.*, 1983). It has been speculated that this expansion might give rise to the changes observed in the elastic constant. These ideas are at this writing, being tested by using molecular dynamics studies (Schuller and Rahman, 1983).

Another possible explanation is the electronic contribution to the elastic moduli. One possible mechanism is analogous to that proposed (Keyes, 1967) to account for effects due to free carriers in semiconductors. The argument is that when a phonon modulates the band structure of a material, thereby lifting certain degeneracies, it allows a redistribution of electrons or holes. This redis-

tribution reduces the free energy and thus effectively lowers the elastic constant. Since degeneracies and a high density of states are most likely to occur either at the boundary or at the center of the Brillouin zone, we would expect a large contribution only if the Fermi energy lies close to one of these regions of the Brillouin zone. A very simple argument shows that the Fermi energy will be folded with a periodicity

$$k_F = n2\pi/d, \tag{6}$$

where k_F is the Fermi wave vector, n an integer, and d is the layer thickness. With the value $k_F = 1.36$ Å^{-1} for Cu, the three lowest solutions are for $2d =$ 9.2, 18.3, and 27.6 Å. This is to be compared to Fig. 14, in which there is only one experimentally observed dip at $2d = 21$ Å, which makes this explanation improbable. In addition a complete check of this simple argument is not possible without a full band structure calculation for such a layered material. Such calculations are extremely time-consuming and expensive due to the large number of atoms in a unit cell.

A third explanation for the decrease in Cu, which has already been alluded to, can be proposed by noting from Figs. 9 and 13 that at the thickness at which the elastic constant has its minimum, the temperature coefficient of resistivity

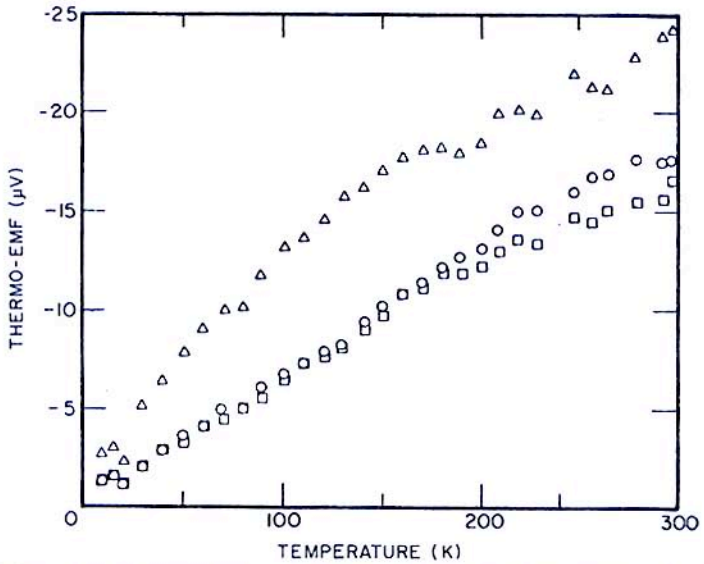

Fig. 14. Thermoelectric power versus temperature for a Cu–Ni sample of modulation wavelength 17 Å. The three sets of data correspond to the sample as prepared with modulation amplitude $A = 0.32$ (□), the sample after being partially annealed to reduce the modulation amplitude to $A = 0.24$ (○), and the sample after being fully annealed to produce a uniform alloy (△) (Schuller *et al.*, 1979).

changes from positive to negative (Werner *et al.*, 1982). This change in sign has been attributed to three-dimensional localization (Abrahams *et al.*, 1979; Imry, 1981) and electron–electron correlation effects (Altshuller and Aronov, 1979; Imry, 1981) as a function of layer thickness. Here, the opening up of a Coulomb correlation gap at E_F would be reflected in an effect on the elastic constants of the material. This explanation is qualitatively similar to that for binary alloys, in which changes in the lattice parameters and crystal structure are attributed to an energy-gap opening up at the Fermi surface when it touches the Brillouin zone. [See Kittel (1957). We are grateful to F. Blatt for pointing this out to us.] A fourth explanation has been advanced in the literature (Chaikin, 1978). In this, the changes in the elastic constants are due to singularities of the dielectric function due to Fermi surface nesting or dimensional effects. Although this explanation is obvious and might seem attractive at first sight, further evidence is needed to substantiate the existence of low-dimensionality behavior in these materials. In addition, it is not clear how these ideas would explain the observed metal–insulator transition.

D. Other Transport Properties (Thermopower, Magnetoresistance, and Hall Effect)

In addition to resistivity, other electronic transport properties such as thermopower and Hall effect should provide important information on the electronic density of states near the Fermi energy in these materials. However, to date there have been only a few reports of such measurements. The problem perhaps lies in the fact that while in principle the thermopower F (within the free-electron model) is simply related to the Fermi energy through

$$F = -2k_B^2 T/|e|E_F, \tag{7}$$

in practice the situation is much more complicated [see, for example, Barnard (1972)]. In the next-higher degree of approximation when real metals properties are included, Eq. (7) is modified by an additional factor that contains details of the shape of the Fermi surface. In particular, the thermopower is related to the energy derivative of the mean free path. While a great deal of progress has been made in understanding thermopower measurements on pure simple metals, the situation is not so clear for many of the more complicated materials (such as alloys) (Barnard, 1972).

The first measurements of thermopower of a series of compositionally modulated metallic films used Cu–Ni (Schuller *et al.*, 1979). In this material there is a large degree of intermixing due to the mutual solubilities of Cu and Ni. Consequently, a composition modulation exists, although the constituent layers are not perfectly defined and, indeed, for some purposes the interfaces can be thought of as an alloy. For thinner-layer samples there is no portion of the material that contains the pure constituent elements, and the entire sample

is a composition modulated alloy (CMA). When thermopower measurements on this particular material are viewed in this way, it is perhaps not surprising that they are not easy to interpret.

As shown in Fig. 14 it was found for Cu–Ni samples with modulation wavelength 17 Å and two different modulation amplitudes (plus a fully annealed sample) measured over the temperature range 20–300 K that the thermopower was larger than that of a pure Cu film made under the same deposition conditions. Thinking of the fully annealed sample as having zero modulation amplitude, an effect was also noted for the thermopower to increase with decreasing amplitude. This is consistent with the idea that most of the temperature dependence of the thermopower comes from impurities.

The effect of varying the composition wavelength on the thermopower of composition-modulated Cu–Ni films was reported by Baral and Hilliard (1979). Here freestanding films approximately 2 μm thick were evaporated and the thermopower relative to pure Cu measured by holding one end of the sample at 0°C and varying the other end between 10 and 200°C in a dc fashion. In agreement with the earlier studies (Schuller *et al.*, 1979), they also found the thermopowers of the composition-modulated and fully annealed samples to be greater than that of pure Cu. In addition, several films with different initial wavelengths were fully annealed and found to give approximately the same thermopowers. By assuming a linear relationship between thermopower and composition amplitude, all samples were normalized to the same amplitude of 0.25, where 1.00 corresponds to full modulation. The result is shown in Fig. 15. A broad maximum located at approximately 20 Å coincides with the point at which the biaxial modulus measured by this same group was found to exhibit a maximum. The conclusion of these latter thermopower measurements was that a critical wavelength exists in composition-modulated Cu–Ni foils. However, we should point out that the existence of a critical wavelength as determined by elastic constant measurements is the subject of some controversy. This result was confirmed independently by Young and torsional moduli (Testardi *et al.*, 1981) measurements, in contrast to the findings of Berry and Pritchet (1976) and those of Itozaki (1981).

Resistivity and magnetoresistance of two composition-modulated Cu–Ni films as well as a fully annealed film have also been reported (Schuller *et al.*, 1979). The magnetoresistance of the sample with the highest degree of composition modulation as well as that of the fully annealed sample (lowest degree of composition modulation) was linear and negative at low fields (<50 kG), finally becoming positive at high fields. This behavior is typical of a ferromagnet. In contrast, the sample with intermediate composition modulation amplitude was quadratic at low fields (<10 kG), becoming linear at higher fields up to the maximum measured of 70 kG. This is typical of a two-band metal below saturation. The Hall coefficient of all three samples was typical of pure Ni. The complicated behavior of the transport properties has been briefly addressed by theoretical band structure calculations (Pickett, 1982).

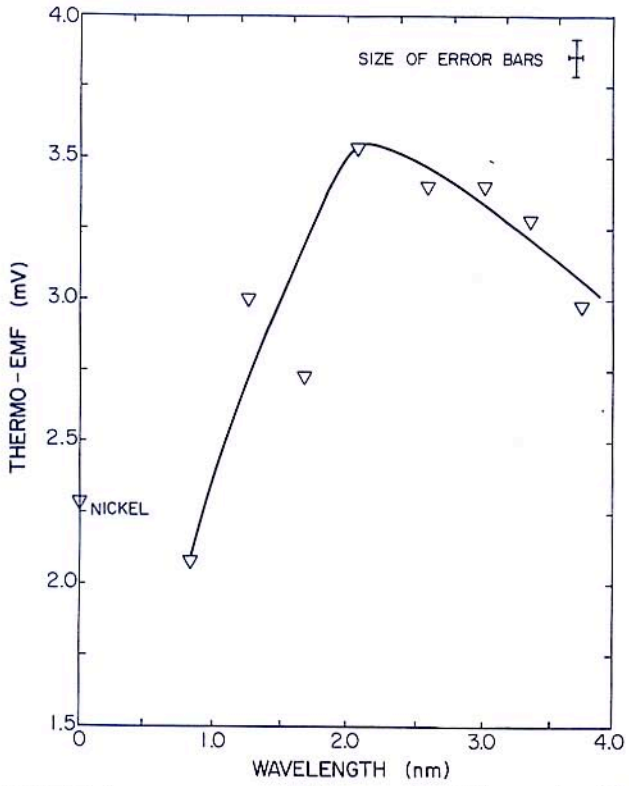

Fig. 15. Thermoelectric power versus modulation wavelength for a series of Cu–Ni samples normalized to the same composition amplitude of $A = 0.25$. [From Baral and Hilliard (1979).]

V. MAGNETIC PROPERTIES

A. Cu–Ni

The first magnetic measurements on compositionally modulated materials were those of Hirsch *et al.* on Cu–Ni in 1964 (Hirsch *et al.*, 1964; Hirsch, 1965). They produced films of individual layer thickness ~10–1000 Å by evaporation and measured the coercive force. They were interested in the behavior of individual thin Ni films but showed that interactions between the Ni layers could not be neglected. About the same time, several groups (Clow, 1962; Friedaender *et al.*, 1965) showed interest in layered samples formed by alternating an alloy of 80% Ni–20% Fe with SiO. It was found (Clow, 1962) that these materials had much lower domain wall coercivities than the pure Ni–Fe alloy.

When discussing the magnetic properties of these composition-modulated materials, it is useful to keep in mind two questions that many of the studies are

implicitly addressing: (1) Can layering produce altered electronic properties such that the magnetization of one of the components is enhanced over the value of the pure material? (2) What coupling, if any, exists between the magnetic layers: direct exchange, dipole, or RKKY? Also, it is important to keep in mind whether the possibility of clustering one or both of the component materials has been conclusively ruled out, and if not, how this can affect the conclusions.

Recently, Thaler *et al.* (1978) examined the behavior of compositionally modulated materials of Cu – Ni. One sample ~4500 Å thick containing approximately 41-at. % Ni and with modulation wavelength of about 30 Å was prepared. X-ray measurements showed one central peak (note that the lattice constants of Cu and Ni are almost identical) flanked on both sides by a sidelobe due to the composition modulation. An analysis of this x-ray measurement indicated an essentially sinusoidal composition modulation of amplitude 0.41 ± 0.06-at. % fraction.

A ferromagnetic resonance (FMR) technique was used to study this sample since this should be sensitive to the local magnetization density $M(z)$, where z is the distance into the sample. It was argued that since $M(z)$ should be an oscillatory function, it would probably be essentially zero in the Cu-rich regions, thereby reducing the average magnetization of the sample. Thus a local probe was necessary to look for any possible effects of the composition modulation on the magnetization of Ni. The original interpretation (Thaler *et al.*, 1978) of these FMR measurements was that at temperatures below approximately 180 K the magnetization of the Ni atoms within each layer was *greater* than that of bulk Ni at 0 K. This observation stimulated further experimental and theoretical investigations of the Cu – Ni system, including static magnetization measurements, neutron scattering, band structure calculations as well as reinterpretations of the original FMR results.

White and Herring (1980) showed that an *apparent* enhancement of the magnetization could arise in a modulated system given a complex distribution of the magnetization within a layer. However, this mechanism is apparently not responsible for the behavior of Cu – Ni, and it is now generally agreed that the magnetization of the Ni is *reduced* rather than enhanced.

Jarlborg and Freeman (1980) performed a self-consistent band structure calculation of the magnetization of a layered Ni – Cu sample. The geometry chosen for the calculation consisted of three atomic layers each of Cu and Ni growing with the [1 1 1] direction perpendicular to the substrate. Due to the large unit cell of this system, only one geometry was calculated. However, the results are of great interest. Jarlborg and Freeman found that the Ni atoms in the center of their layers suffered a small reduction in moment below the value of pure Ni ($0.54\mu_B$) while the interface Ni atoms experienced a much larger reduction to $0.37\mu_B$.

Gyorgy *et al.* (1980, 1982) repeated the FMR measurements on a number of

Cu–Ni samples of various layer thicknesses. They also measured the average magnetization by using a vibrating sample magnetometer as well as a force method. Figure 16 shows the average magnetization as a function of inverse layer thickness. Since both the magnetization and the anisotropy field depend only on the Ni thickness and not on the Cu thickness, they concluded that the intrinsic Ni properties are not determined by modulation effects. Also, the absence of superparamagnetic effects led Gyorgy *et al.* to conclude that if the Ni were in clusters in their samples, the minimum size of such clusters was approximately $10 \times 200 \times 200$ Å.

There are two possible reasons for the behavior shown in Fig. 16 of the average magnetization as the thickness is reduced. Either the magnetization of the Ni decreases with layer thickness, or there are dead layers of nonmagnetic

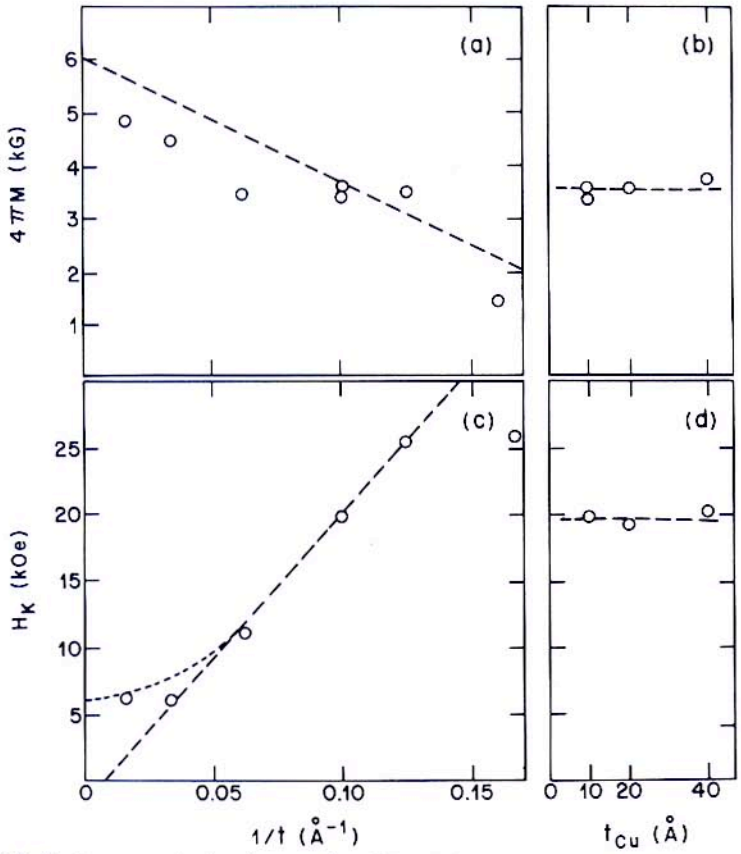

Fig. 16. Static magnetization for a series of Cu–Ni compositionally modulated films. (a) $t_{Ni} = t_{Cu} = t$; (b) $t_{Ni} = 10$ Å; (c) $t_{Ni} = t_{Cu} = t$; (d) $t_{Ni} = 10$ Å. [From Gyorgy *et al.* (1980).]

Ni at the Ni–Cu interfaces. The data of Gyorgy *et al.* did not allow them to unambiguously choose between the two options, but Gyorgy *et al.* speculated that the amplitude of the composition modulation in their films suggested that the reduced magnetization was a better explanation.

Direct current magnetization measurements of Cu–Ni samples as a function of temperature, magnetic field, composition wavelength, and composition amplitude have also been reported (Zheng *et al.*, 1981, 1982). The results found for these samples were that the maximum magnetization was 0.36 μ_B/Ni atom, in agreement with neutron scattering results (Felcher *et al.*, 1980) and with band structure calculations (Jahlborg and Freeman, 1980). Evidence for Ni clustering within the layers was also found.

Polarized neutron scattering (Felcher *et al.*, 1980) has been used to determine the average Ni moment as well as the moment fluctuations about the average for a sample of composition modulation wavelength 22 Å and average composition $Ni_{0.4}Cu_{0.6}$. The maximum low-temperature magnetization found was approximately 0.3 μ_B/Ni atom, in agreement with dc measurements (Gyorgy *et al.*, 1980, 1982; Zheng *et al.*, 1981a, 1982) and with band structure calculations (Jahlborg and Freeman, 1980). From the size of the moment fluctuations, it was concluded that the Ni in this sample tended to form clusters. The size of the clusters varied from about 50 Ni atoms in the Ni-rich regions of the sample to about 20 Ni atoms in the Cu-rich regions.

Work by the Northwestern group on Cu–Ni has also used a torque magnetometer and a superconducting quantum interference device (SQUID) susceptometer in addition to the FMR technique (Flevaris *et al.*, 1982b). They found agreement among all three techniques at room temperature. For one sample consisting of alternating three atomic planes of Ni-rich layers with six atomic planes of Cu-rich layers, they found a magnetization that increased linearly as the temperature was reduced. This was interpreted as evidence for two-dimensional ferromagnetism. However, given the considerable structural data on similarly prepared films, which show large amounts of interdiffusion and clustering (Gyorgy *et al.*, 1980, 1982; Zheng *et al.*, 1981a, 1982; Felcher *et al.*, 1980), further work is clearly needed before such an interpretation can be considered conclusive for this system.

A basic problem in interpreting static magnetization measurements on these materials is that it is not known how the composition modulation might affect some of the average properties. In a model calculation of the effect of composition modulation on the Curie temperature T_c of a modulated sample, Jones (1982) found that Arrot plots led to T_c's that were essentially (within 4%) those corresponding to the maximum T_c of the sample (T_c^{max}), rather than to some average T_c. He found that only the upper 40% of the magnetic composition, i.e., that portion of each layer with the largest magnetic concentration, contributed to T_c^{max}. This is a very useful result for interpreting static magnetization measurements on these materials.

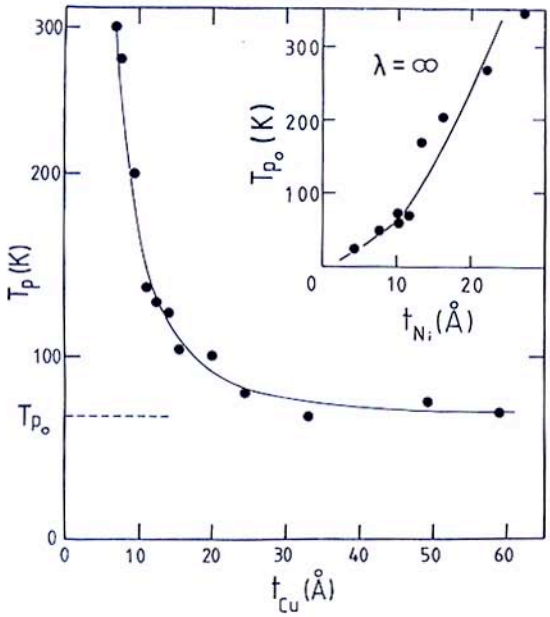

Fig. 17. Temperature of the peak in the ac susceptibility T_p versus thickness of the Cu layer for a series of Ni–Cu samples. [From Zhou *et al.* (1981). Copyright 1981 North-Holland Publishing Co. Amsterdam.]

In measurements of the low-field ac susceptibility on a number of Cu–Ni samples of differing wavelengths, Zhou *et al.* (1981) found a peak in the susceptibility as a function of temperature. The dependence of the magnetic transition temperature (as they defined it by the peak in the susceptibility) on the wavelength of the composition modulation is shown in Fig. 17. In this experiment, Zhou *et al.* kept the average thickness of a Ni layer constant at 10 Å and varied the Cu thickness to alter the modulation wavelength. Their conclusion was that they could not account for the dependence of the peak in the temperature dependence of the ac susceptibility on modulation wavelength if the magnetization density of the Ni planes were uniform. For this reason they feel that the indirect RKKY exchange between Ni layers must be responsible. They also conclude that there is not an extensive (>4-Å) magnetically dead Ni region in these samples. However, the issue of possible clustering in these samples as well as possible shorts connecting adjacent Ni layers and how this would affect the results was not directly addressed.

B. Magnetic Properties of Other Materials

While to date Cu–Ni has been the most extensively studied magnetic modulated material, there have been measurements reported on several other sys-

tems. Preliminary attempts have been made to alter the number of itinerant d electrons per atoms in Mn, and thereby to alter its magnetic properties, by alternately layering Mn with Ni and Co (Stearns, 1982). The measurements to date indicate that the materials exhibit a wide variety of complicated magnetic behavior. Part of this is probably due to the various crystallographic orientations obtained for different layer thicknesses. This points out the need for better control over the crystal growth of these materials for a number of studies, as well as very thorough sample characterization.

A torque magnetometer was used by the Northwestern University group to determine the magnetization density and first-order uniaxial anisotropy constant for a series of PD–Ni films (Flevaris *et al.*, 1982a). In general the number of Pd and Ni atoms in each layer was not identical for these studies. It was concluded that for samples with very few atoms per layer (<7) the magnetization density per Ni atom became greater than that of pure Ni. This effect was found to be as large as 25% for the thinnest layer samples studied and was attributed to different exchange-enhanced susceptibilities of Pd in the different local environments of the sample. However, when dealing with samples that contain an *average* of 3 or 4 atoms per layer, sample characterization is critical. It should be kept in mind that the standard $\theta-2\theta$ Bragg diffraction with the scattering vector perpendicular to the films is sensitive *only* to structure perpendicular to the film. Structural differences within a layer (such as clustering) cannot be detected in this way.

Data on the magnetic properties of CMAs incorporating hydrogen have also been reported (Flevaris *et al.*, 1981). Unfortunately, the hydrogen was incorporated at room temperature and quantitative measurements of the amounts remaining after charging the samples were not given, nor were details given of the possible damage the electrolytically incorporated hydrogen caused. Considerable amounts of ac susceptibility and FMR data have been taken on these materials; however, the theories needed to interpret these data contain a number of adjustable parameters. Given that sample characterization is incomplete and given the complex nature of the materials, no clear conclusions can be drawn from these particular measurements. A general comment would be that much more work is needed on "simple" modulated metals before more complex materials can be fruitfully studied.

VI. SUMMARY

The study of electronic and magnetic properties of metallic superlattices is not yet as developed as the study of physical properties of semiconductor superlattices. Much progress has been made in just the past few years, but metallic samples do not yet exhibit the same degree of long-range structural coherence perpendicular to the layers. However, the several metallic systems

that have been successfully prepared show a number of interesting physical properties. Transport properties have been shown to be related to elastic properties, and the usefulness of these materials for studying phenomena such as two-dimensional magnetism is now apparent. Judging from the rapid progress made in the past few years in studying electronic and magnetic properties of these materials, the next few years should lead to a number of discoveries.

We have made every attempt to make this chapter a comprehensive review (up to the submission date of Fall 1982) but, as in every rapidly developing field, it is inevitable that some work has escaped our attention. We offer our apologies to our colleagues in this field whose work may not have been covered.

ACKNOWLEDGMENTS

We would like to thank our collaborators who contributed to various aspects of the work described here: I. Banerjee, C. Chun, G. P. Felcher, M. Grimsditch, R. T. Kampwirth, J. B. Ketterson, M. R. Khan, A. Kueny, K. Meyer, A. Rahman, S. K. Sinha, J. Vicent, T. R. Werner, Q. S. Yang, G. G. Zheng, and J. Q. Zheng.

This work was supported by the U.S. Department of Energy and the Office of Naval Research under grant No. N00014-83-F-0031.

REFERENCES

Abrahams, E., Anderson, P. W., Licciardello, D. C., and Ramakrishnan, T. V. (1979). *Phys. Rev. Lett.* **42,** 673.

Altshuller, B. L., and Aronov, A. G. (1979). *Zh. Eksp. Teor. Fiz.* **77,** 2028 [*Sov. Phys.-JETP (Engl. transl.)* **50,** 968 (1979).]

Banerjee, I., Yang, Q. S., Falco, C. M., and Schuller, I. K. (1982). *Solid State Commun.* **41,** 805.

Baral, D., and Hilliard, J. E. (1979). *Appl. Phys. Lett.* **41,** 156.

Barnard, R. D. (1972). "Thermoelectricity in Metals and Alloys," Taylor and Francis, London.

Berry, B. S., and Pritchet, W. C. (1976). *Thin Solid Films* **33,** 19.

Calverly, A., and Rose-Innes, A. C. (1960). *Proc. R. Soc. London* **255A,** 267.

Chaikin, P. M. (1978). *Ann. N.Y. Acad. Sci.* **128,** 127.

Clow, H. (1962). *Nature* **194,** 1035.

Cook, H. E., and Hilliard, J. E. (1969). *J. Appl. Phys,* **40,** 2191.

Dinklage, J. B. (1967). *J. Appl. Phys.* **38,** 3781.

Dinklage, J., and Frerichs, R. (1963). *J. Appl. Phys.* **34,** 2633.

DuMond, J., and Youtz, J. P. (1940). *J. Appl. Phys.* **11,** 357.

Durbin, S. M., Cunningham, J. E., Mochel, M. F., and Flynn, C. P. (1981). *J. Phys. F* **11,** L223.

Durbin, S. M., Cunningham, J. E., and Flynn, C. P. (1982). *J. Phys. F* **12,** L75.

Dynes, R. C. (1982). *Surf. Sci.* **113,** 510.

Elliott, R. P. (1965). "Constitution of Binary Alloys," 1st supplement, McGraw-Hill, New York.

Falco, C. M., and Schuller, I. K. (1982a). *In* "Novel Materials and Techniques in Condensed Matter" (G. W. Crabtree and P. Vashishta, eds.), p. 21, North-Holland Publ., New York.

Falco, C. M., and Schuller, I. K (1982b). *In* "Proceedings of IV Conference on Superconductivity in d- and f-band Metals" (W. Weber and W. Buckel, eds.), p. 283. Kernsforschungsanlage, Karlsruhe, Federal Republic of Germany.

Farnell, G. W. (1969). *In* "Physical Acoustics" (W. P. Mason and R. N. Thurston, eds.), Vol. 6, p. 109, Academic Press, New York.

Felcher, G. P., Cable, J. W., Zheng, J. Q., Ketterson, J. B., and Hilliard, J. E. (1980). *J. Mag. Mag. Mater.* **21,** L198.
Flevaris, N. K., Baral, D., and Hilliard, J. E. (1981). *In* "Metal Hydrides" (G. Bambakidis, ed.), p. 301, Plenum, New York.
Flevaris, N. K., Ketterson, J. B., and Hilliard, J. E. (1982a). *J. Appl. Phys.* **53,** 2439.
Flevaris, N. K., Ketterson, J. B., and Hilliard, J. E. (1982b). *J. Appl. Phys.* **53,** 8046.
Friedlaender, F. J., Kneller, E., and Silva, I. F. (1965). *IEEE Trans. Magn.* **MAG-1,** 251.
Geerk, J., Gurvitch, M., McWhan, D. B., and Rowell, J. M. (1982). *Physica B + C* **109-110,** 1772.
Gyorgy, E. M., Dillon, J. F., Jr., McWhan, D. B., Rupp, L. W., Jr., Testardi, L. R., and Flanders, P. J. (1980). *Phys. Rev. Lett.* **45,** 57.
Gyorgy, E. M., McWhan, D. B., Dillon, J. F., Jr., Walker, L. R., and Waszczak, J. V. (1982). *Phys. Rev. B* **25,** 6539.
Hamelin, B. (1976). *Nucl. Instrum. Meth.* **135,** 299.
Hansen, M. and Ankerko, K. (1958). "Constitution of Binary Alloys," 2nd ed., McGraw-Hill, New York.
Hertel, G., McWhan, D. B., and Rowell, J. M. (1982). *In* "Proceedings of IV conference on Superconductivity in d- and f- band Metals" (W. Weber, and W. Buckel, eds.) p. 299. Kernsforschungsanlage, Karlsruhe, Federal Republic of Germany.
Hirsch, A. A. (1965). *IEEE Trans. Magn.* **MAG-1,** 254.
Hirsch, A. A., Friedman, N., and Eliezer, Z. (1964). *Physica* **30,** 2314.
Imry, Y. (1981). *J. Appl. Phys.* **52,** 1817.
Ioffe, A. F., and Regel, A. R. (1960). *Prog. Semicond.* **4,** 237.
Itozaki, H. (1981). Ph.D. thesis, Northwestern Univ., Evanston, Illinois.
Jahlborg, T., and Freeman, A. J. (1980). *Phys. Rev. Lett.* **45,** 653.
Jones, W. R. (1982). *J. Appl. Phys.* **53,** 2442.
Kaveh, M., and Mott, N. F. (1981). *J. Phys. C* **14,** L183, L177.
Keyes, R. W. (1967). *Solid State Phys.* **20,** 37.
Khan, M., Chun, C. S. L., Felcher, G., Grimsditch, M., Kueny, A., Falco, C. M., and Schuller, I. K. (1983). *Phys. Rev. B* **27,** 7186.
Kittel, C. (1957). "Introduction to Solid State Physics," 2nd ed., p. 322, Wiley, New York.
Kueny, A., Grimsditch, M., Miyano, K., Banerjee, I., Falco, C. M., and Schuller, I. K. (1982). *Phys. Rev. Lett.* **48,** 166.
Lowe, W. P., Barbee, T. W., Jr., Geballe, T. H., and McWhan, D. B. (1981). *Phys. Rev. B* **24,** 6193.
Lynn, J. W., Knems, J. K., Pasell, L., Saxena, A. M., and Schoenborn, B. P. (1976). *J. Appl. Crystallogr.* **9,** 454.
Mayadas, A. F., and Shatzkes, M. (1970). *Phys. Rev. B* **1,** 1382.
Moffatt, G. (1981). "Handbook of Binary Phase Diagrams," General Electric Co., Schenectady, New York.
Mott, N. F. (1969). *Philos. Mag.* **19,** 835.
Paulson, W. M., and Hilliard, J. E. (1977). *J. Appl. Phys.* **48,** 2117.
Pickett, W. E. (1982). *J. Phys. F* **12,** 2195.
Roll, K., and Reill, W. (1982). *Thin Solid Films* **89,** 221.
Ruggiero, S. (1981). Ph.D. thesis, Stanford Univ., Stanford, California.
Rytov, S. M. (1956). *Akust. Zh.* **2,** 71 [*Sov. Phys.-Acoust. (Engl. transl.)* **2,** 67 (1956).]
Saxena, A. M., and Schoenborn, B. P. (1977a). *Acta. Crystallogr. A* **33,** 805.
Saxena, A. M., and Schoenborn, B. P. (1977b). *Acta. Crystallogr. A* **33,** 813.
Schuller, I. K. (1980). *Phys. Rev. Lett.* **44,** 1597.
Schuller, I. K., and Falco, C. M. (1980). *In* "Inhomogeneous Superconductors–1979" (D. U. Gubser, T. L. Francavilla, J. R. Leibowitz, and S. A. Wolf, eds.), p. 197, American Institute of Physics, New York.
Schuller, I. K., and Falco, C. M. (1982). *Surf. Sci.* **113,** 443.

Schuller, I. K. and Rahman, A. (1983). *Phys. Rev. Lett.* **50,** 1377.
Schuller, I. K., Falco, C. M., Thaler, B., Ketterson, J. B., and Hilliard, J. (1979). *In* "Modulated Structures" (J. M. Cowley, J. B. Cohen, M. B. Salamon, and B. J. Wuensch, eds.), p. 417, American Institute of Physics, New York.
Shunk, F. A. (1969). "Constitution of Binary Alloys," 2nd supplement, McGraw-Hill, New York.
Spiller, E. (1981). *In* "Low Energy X-Ray Diagnostics—1981" (D. T. Attwood and B. L. Henke, eds.), p. 124, American Institute of Physics, New York.
Stearns M. B. (1982). *J. Appl. Phys,* **53,** 2436.
Testardi, L. R., Willens, R. H., Krause, J. T., McWhan, D. B., and Nakaha, S. (1981). *J. Appl. Phys.* **52,** 510.
Thaler, B. J., Ketterson, J. B., and Hilliard, J. E. (1978). *Phys. Rev. Lett.* **41,** 336.
Werner, T. R., Banerjee, I., Yang, Q. S., Falco, C. M., and Schuller, I. K. (1982). *Phys. Rev. B* **26,** 2224.
White, R. M., and Herring, C. (1980). *Phys. Rev. B* **22,** 1465.
Zheng, J. Q., Falco, C. M., Ketterson, J. B., and Schuller, I. K. (1981a). *Appl. Phys. Lett.* **38,** 424.
Zheng, J. Q., Ketterson, J. B., Falco, C. M., and Schuller, I. K. (1981b). *Physica B + C* **108,** 945.
Zheng, J. Q., Ketterson, J. B., Falco, C. M., and Schuller, I. K. (1982). *J. Appl. Phys.* **53,** 3150.
Zhou, W. S., Wong, H. K., Owers-Bradley, J. R., and Halperin, W. P. (1981). *Physica* **108B,** 953.